Histol Histopathol (2023) 38: 53-64

**http://www.hh.um.es**

Histology and Histopathology
*From Cell Biology to Tissue Engineering*

**ORIGINAL ARTICLE** **Open Access**

# Circ_0067717 promotes colorectal cancer cell growth, invasion and glutamine metabolism by serving as a miR-497-5p sponge to upregulate SLC7A5

**Mo Song and Jipan Liu**

Department of Anorectal Surgery, Hengshui People's Hospital, Hengshui, China

**Summary.** Background. Circular RNAs (circRNAs) have been shown to exert vital functions in colorectal cancer (CRC) development. However, the role of circ_0067717 in CRC progression remains to be elucidated.

Methods. The expression of circ_0067717, microRNA (miR)-497-5p and solute carrier family 7 member 5 (SLC7A5) was analyzed by quantitative real-time PCR. Cell proliferation, apoptosis and invasion were determined by cell counting kit 8 assay, EdU assay, flow cytometry and transwell assay. Protein expression was examined using western blot analysis. Glutamine metabolism was assessed by measuring glutamine consumption, α-ketoglutarate production and glutamate production. The interaction between miR-497-5p and circ_0067717 or SLC7A5 was identified by dual-luciferase reporter assay. Xenograft tumor models were constructed to confirm the role of circ_0067717 in CRC tumorigenesis *in vivo*.

Results. Our data revealed that circ_0067717 was upregulated in CRC tissues and cells, and its knockdown restrained CRC cell proliferation, invasion, glutamine metabolism, and promoted apoptosis. MiR-497-5p was lowly expressed in CRC and it could be sponged by circ_0067717. MiR-497-5p inhibitor eliminated the regulation of circ_0067717 knockdown on CRC cell function. SLC7A5 was targeted by miR-497-5p and was positively regulated by circ_0067717. MiR-497-5p overexpression suppressed CRC cell growth, invasion and glutamine metabolism, and SLC7A5 was able to revoke this effect. Animal experiments showed that interference of circ_0067717 reduced CRC tumor growth.

Conclusion. Our research pointed out that circ_0067717 facilitated CRC development depending on the regulation of the miR-497-5p/SLC7A5 axis, providing a novel insight into CRC treatment.

**Key words:** Colorectal cancer, circ_0067717, miR-497-5p, SLC7A5

*Corresponding Author:* Mo Song, Department of Anorectal Surgery, Hengshui People's Hospital, No. 180, Renmin East Road, Taocheng District, Hengshui 053000, China. e-mail: songmo_000@163.com

DOI: 10.14670/HH-18-494

## Introduction

Colorectal cancer (CRC), has the characteristics of high morbidity and high mortality, is a common malignant tumor (Arnold et al., 2017; Araghi et al., 2019). Although much progress has been made in cancer treatment, CRC patient prognosis has not been significantly improved (Carlomagno et al., 2019; Shan et al., 2019). Molecular targeted therapy is one of the treatment methods of CRC, which achieves the purpose of suppressing cancer by specifically inhibiting or promoting some molecular targets (Piawah and Venook, 2019; Geng et al., 2017). In order to develop new treatments for CRC, it is important to investigate new molecular targets that regulate CRC progression.

Circular RNAs (circRNAs) are non-coding RNA molecules with circular structure, which are highly conserved (Kristensen et al., 2019). Importantly, circRNA was found to contain microRNA (miRNA) response elements, which can competitively bind miRNA to remove the regulation of miRNA on downstream genes (Panda, 2018; Misir et al., 2020). CircRNA role in the progression of human diseases has been gradually revealed, especially in cancer (Li et al., 2020). Existing studies have shown that circRNAs are promising tumor biomarkers for the clinical diagnosis and treatment of cancer because of their high stability in the body (Li and Han, 2019; Wang et al., 2021). Studies had suggested that circ_0000392 contributed to CRC progression by enhancing cell proliferation and invasion through the miR-193a-5p/PIK3R3 pathway (Xu et al., 2020). Also, circ_002144 had been confirmed to regulate miR-615-5p/LARP1 axis to promote cell proliferation and metastasis (Wu et al., 2021).

Through RNA deep sequencing, Ge et al. found a

total of 67 differentially expressed circRNA in CRC tissues and normal tissues (Ge et al., 2019). Among the top 10 upregulated circRNAs, we found that the function of highly expressed circ_0067717 in CRC progression has not been studied so far. A previous study showed that circ_0067717 was overexpressed in HBV-associated hepatocellular carcinoma tissues and could facilitate cell proliferation and metastasis (Chen et al., 2021). Therefore, we speculated that the upregulated circ_0067717 in CRC tissues might contribute to the malignant phenotype of CRC. Combined with this hypothesis, we conducted functional tests and explored its potential molecular mechanism, hoping to offer a potential new target for CRC treatment.

## Materials and methods

### *Patient samples*

34 CRC patients were recruited from Hengshui People's Hospital and signed written informed consent for our study. The clinicopathologic features of CRC patients are listed in Table 1. After surgery, CRC tumor tissues (n=34) and adjacent normal tissues (n=34) were collected and stored at -80°C for later use. Our research was approved by the Ethics Committee of the Hengshui People's Hospital and was performed in accordance with the Declaration of Helsinki.

### *Cell culture and transfection*

Human CRC cells (SW480, SW620, LoVo and HCT-116) and normal colon cells (NCM460) were bought from Biovector NTCC (Beijing, China) and were cultured in DMEM medium (Gibco, Carlsbad, CA, USA) containing 10% FBS (Gibco) and 1% penicillin/streptomycin (Gibco) at 37°C with 5% $CO_2$.

**Table 1.** Relationship between circ_0067717 expression and clinicopathologic features of colorectal cancer patients.

| | Characteristics | circ_0067717 expression | |
|---|---|---|---|
| | n=34 | Low(n=17) | High(n=17) |
| Gender | | | |
| Female | 16 | 7 | 9 |
| Male | 18 | 10 | 8 |
| Age (years) | | | |
| ≤60 | 14 | 6 | 8 |
| >60 | 20 | 11 | 9 |
| TNM grade | | | |
| I+II | 15 | 12 | 3 |
| III+IV | 19 | 5 | 14 |
| Lymph node metastasis | | | |
| Positive | 19 | 4 | 15 |
| Negative | 15 | 13 | 2 |
| Tumor size | | | |
| ≤3 cm | 14 | 11 | 3 |
| >3 cm | 20 | 6 | 14 |

TNM, tumor-node-metas-tasis; *P<0.05.

### *Cell transfection*

Lipofectamine 3000 (Invitrogen, Carlsbad, CA, USA) was used for cell transfection in accordance with the instructions. Circ_0067717 small interfering RNA (si-circ_0067717) or lentivirus short hairpin RNA (sh-circ_0067717), miR-497-5p mimic or inhibitor (anti-miR-497-5p), pcDNA SLC7A5 overexpression vector, and negative controls were synthesized by RiboBio (Guangzhou, China).

### *Quantitative real-time PCR (qRT-PCR)*

After extracting RNA with TRIzol reagent (Invitrogen), RNA (1 μg) was reverse-transcribed into cDNA using PrimeScript RT Reagent Kit (Takara, Dalian, China). After that, SYBR Green (Takara) was mixed with cDNA (2 μL) and specific primers (0.2 μM) for performing PCR in PCR system (Thermo-Fisher Scientific, Waltham, MA, USA). The conditions for PCR were as follows: 95°C for 10 min, 95°C for 10 sec, and 60°C for 60 sec, with a total of 40 cycles. Data were analyzed using $2^{-\Delta\Delta Ct}$ method with β-actin or U6 as internal control. Primer sequences are shown in Table 2. For the verification of circ_0067717, the extracted RNA was hatched with RNase R for 15 min, and then circ_0067717 expression before and after RNase R treatment was measured. In addition, random primers and Oligo $(dT)_{18}$ primers were used during cDNA synthesis, and then PCR was carried out to detect circ_0067717 expression. Here, GAPDH was used as a linear RNA control.

### *Cell counting kit 8 (CCK8) assay*

CRC cells ($5\times10^3$ cells/well) were seeded into 96-well plates and cultured for 48h. Cells were hatched with CCK8 reagent (Dojindo, Kumamoto, Japan) for 4 h. Cell viability was analyzed at 450 nm wavelength using a microplate reader (Thermo-Fisher Scientific).

**Table 2.** Primer sequences used for qRT-PCR.

| Name | | Primers (5'-3') |
|---|---|---|
| circ_0067717 | Forward | CAAGGCAGCCATAGTTCACA |
| | Reverse | ACTTGTGTGGCTGACAGCAT |
| miR-497-5p | Forward | GCCGAGCAGCAGCACACTGTG |
| | Reverse | ATCCAGTGCAGGGTCCGAGG |
| SLC7A5 | Forward | CCGTGAACTGCTACAGCGT |
| | Reverse | CTTCCCGATCTGGACGAAGC |
| GAPDH | Forward | CTCTGCTCCTCCTGTTCGAC |
| | Reverse | CGACCAAATCCGTTGACTCC |
| β-actin | Forward | CTCCATCCTGGCCTCGCTGT |
| | Reverse | GCTGTCACCTTCACCGTTCC |
| U6 | Forward | CTCGCTTCGGCAGCACA |
| | Reverse | AACGCTTCACGAATTTGCGT |

### *EdU assay*

Based on the kit instruction, the EdU positive cell rate of CRC cells was analyzed by EdU Kit (RiboBio). Cell fluorescence was captured under a fluorescence microscope (Olympus Corporation, Tokyo, Japan).

### *Flow cytometry*

Using Annexin V-FITC Apoptosis Detection Kit (Beyotime, Shanghai, China), CRC cells ($1\times10^6$ cells) were treated with Annexin V-FITC and propidium iodide. CytoFLEX flow cytometer (Beckman Coulter, Miami, FL, USA) was used to analyze cell apoptosis rate.

### *Transwell assay*

CRC cells ($4\times10^5$ cells/chamber) with serum-free medium were seeded into the upper of Matrigel pre-coated transwell chambers (BD Biosciences, Franklin Lakes, NJ, USA). Cells were cultured for 24 h under the condition that lower chamber filled with serum medium. Then, cells passed through the membranes were stained by crystal violet and then photographed under microscope (Olympus Corporation). The numbers of invasive cells in five randomly selected visual fields were counted with Image J software.

### *Western blot (WB) analysis*

Total protein was lysed by RIPA lysis buffer (Beyotime) and then quantified by BCA Kit (Beyotime). Protein samples (30 μg) were electrophoresed in SDS-PAGE gel followed by transferral onto PVDF membrane. Membranes were treated with anti-C-myc (1:1,000, ab32072, Abcam, Cambridge, MA, USA), anti-MMP2 (1:1,000, ab97779, Abcam), anti-SLC7A5 (1:3,000, ab99419, Abcam), or anti-β-actin (1:1,000, ab8227, Abcam). After the membrane was hatched with secondary antibody (1:50,000, ab205718, Abcam), protein band was detected with BeyoECL Moon Kit (Beyotime), and relative protein expression was analyzed by ImageJ software.

### *Glutamine metabolism assay*

Glutamine consumption, α-ketoglutarate production and glutamate production were determined by Glutamine Assay Kit, α-ketoglutarate Assay Kit and Glutamate Assay Kit (Abcam) in line with the kit instructions. For detecting glutamine consumption, the supernatant of CRC cells was mixed with Hydrolysis Enzyme Mix and Hydrolysis Buffer for 30 min, and then incubated with Development Buffer, Development Enzyme Mix and Developer for 60 min. The absorbance at 450 nm was detected using a microplate reader (Thermo-Fisher

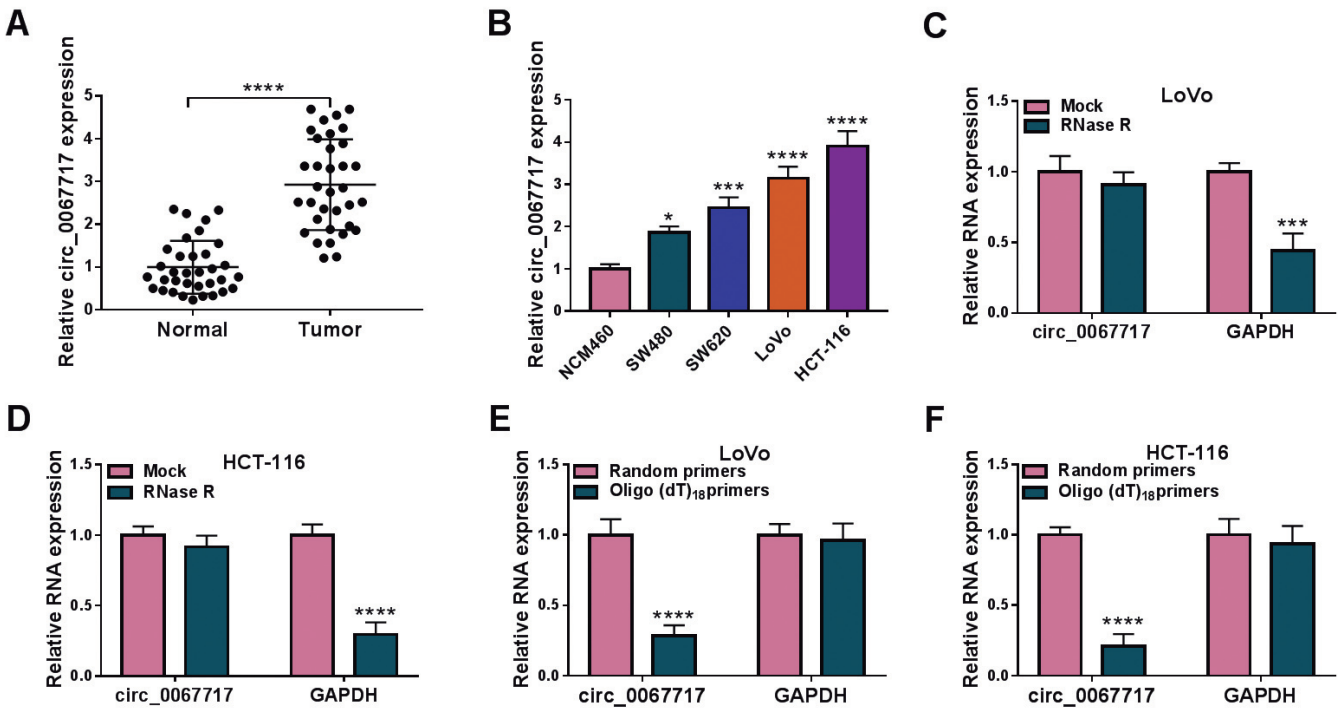


**Fig. 1.** circ_0067717 expression in CRC tumor tissues and cells. **A.** circ_0067717 expression in CRC tumor tissues and adjacent normal tissues was measured by qRT-PCR. **B.** QRT-PCR was used to detect circ_0067717 expression in CRC cells (SW480, SW620, LoVo and HCT-116) and NCM460 cells. RNase R assay **(C, D)** and Oligo $(dT)_{18}$ primers **(E, F)** were used to assess the circular characteristic of circ_0067717. *P<0.05, ***P<0.001, ****P<0.0001.

Scientific). For detecting α-ketoglutarate production, the supernatant of CRC cells was incubated with Alpha KG Assay Buffer, Alpha KG Converting Enzyme, Alpha KG Enzyme Mix and Alpha KG Probe for 30 min followed by measuring the absorbance at 570 nm. For testing glutamate production, the supernatant of CRC cells was incubated with Glutamate Assay Buffer, Glutamate Developer and Glutamate Enzyme Mix for 30 min. Then, the absorbance was analyzed at 450 nm. All data were calculated according to the standard curve, which is explained in the kit instructions.

### *Dual-luciferase reporter assay*

The sequences of circ_0067717 or SLC7A5 3'UTR were inserted into the pmirGLO vector to generate the corresponding wild-type (WT-circ_0067717 or WT-SLC7A5 3'UTR) or mutant-type (MUT-circ_0067717 or MUT-SLC7A5 3'UTR) vectors. CRC cells were seeded into 24-well plates and cultured until 80% confluence. The vectors were transfected into CRC cells with miR-497-5p mimic/miR-NC using Lipofectamine 3000 (Invitrogen) according to the manufacturer's protocol. Relative luciferase activity was the ratio of *Firefly/Renilla*.

### *Mice xenograft models*

HCT-116 cells were stably transfected with sh-circ_0067717/sh-NC for 48 h and then were collected and suspended with PBS. The transfected cells were injected into BALB/c nude mice subcutaneously (n=6/group, right flank; Vital River, Beijing, China). Tumor volume was calculated by detecting tumor length and width every 3 days starting from day 7. After 22 days, mice were sacrificed and the tumor tissue was taken for photographing and weighing. A portion of tumor tissue was used for the detection of target genes,

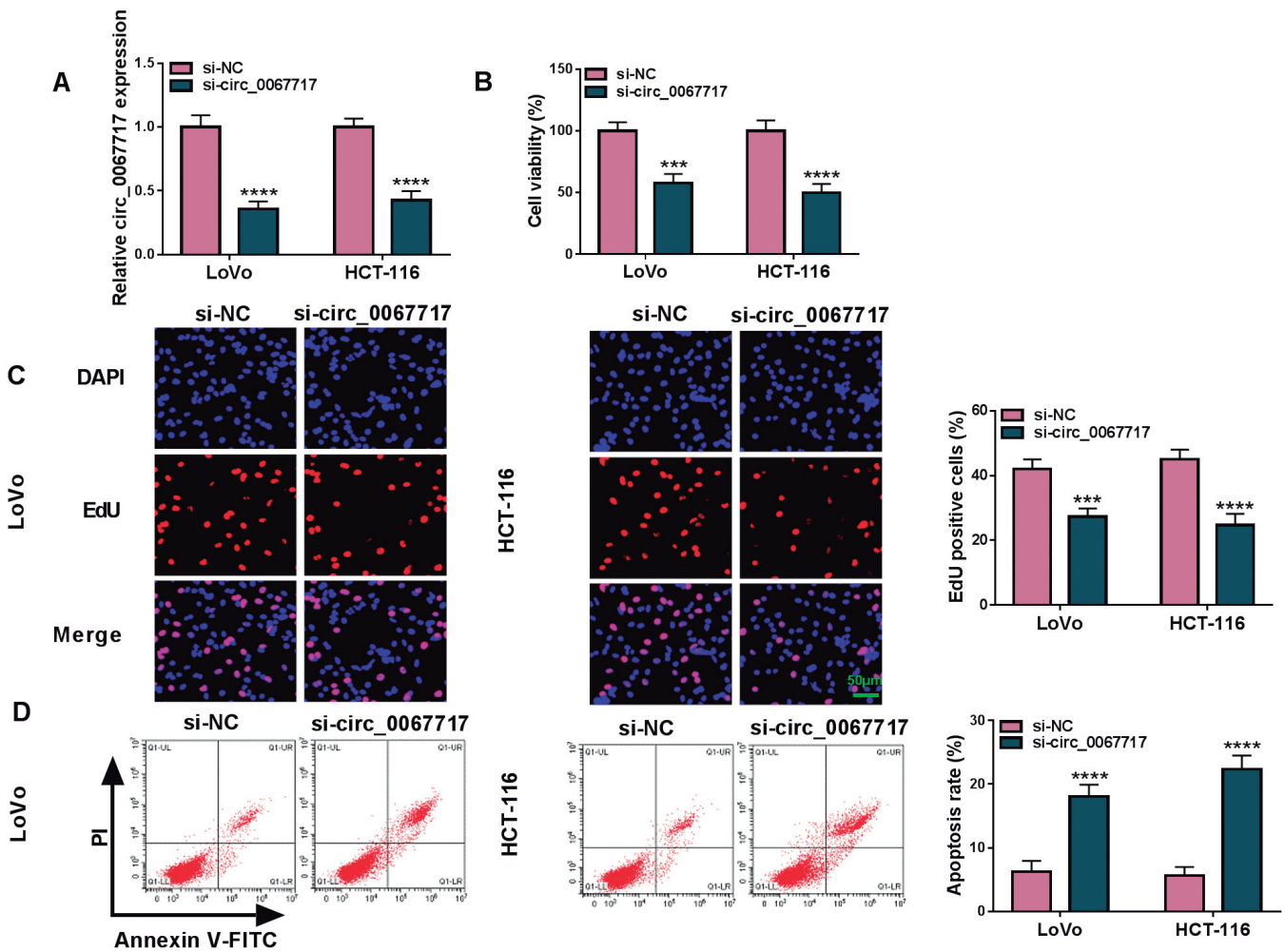


**Fig. 2.** The regulation of si-circ_0067717 on CRC cell proliferation and apoptosis. LoVo and HCT-116 cells were transfected with si-NC or si-circ_0067717. **A.** circ_0067717 expression was detected by qRT-PCR. CCK8 assay **(B)**, EdU assay **(C)** and flow cytometry **(D)** were performed to measure cell proliferation and apoptosis. ***P<0.001, ****P<0.0001.

while the other portion was prepared for paraffin sections to carry out immunohistochemical (IHC) staining. Animal experiments were approved by the Animal Ethics Committee of Hengshui People's Hospital.

### *Statistical analysis*

Data were analyzed by GraphPad Prism 7.0 software and are presented as means ± SD. Linear correlation was compared with Pearson correlation analysis. Student's *t*-test or ANOVA was performed to compare the difference between groups. Statistical significance was deemed as $P<0.05$.

## Results

### *Circ_0067717 expression was upregulated in CRC tumor tissues and cells*

Through measuring circ_0067717 expression, circ_0067717 expression was confirmed to be higher in CRC tumor tissues than in adjacent normal tissues (Fig. 1A). By analyzing the correlation between the expression of circ_0067717 and the clinicopathological features of patients, we found that the high expression of circ_0067717 was related to TNM stage, lymph node metastasis and tumor size of CRC patients (Table 1). Compared to NCM460 cells, the circ_0067717 was also upregulated in four CRC cells (SW480, SW620, LoVo and HCT-116) (Fig. 1B). Then, the RNA from LoVo and HCT-116 cells was treated with RNase R, and then we detected circ_0067717 and linear RNA GAPDH expression. The results showed that circ_0067717 expression was not changed, while GAPDH expression was reduced, confirming that circ_0067717 could resist the digestion of RNase R (Fig. 1C,D). In addition, circ_0067717 could not be amplified by Oligo $(dT)_{18}$ primers, showing that it did not contain poly-A tails (Fig. 1E,F).

### *Knockdown of circ_0067717 inhibited CRC cell growth, invasion and glutamine metabolism*

Then, si-circ_0067717 was used to knockdown circ_0067717 in CRC cells to explore the role of

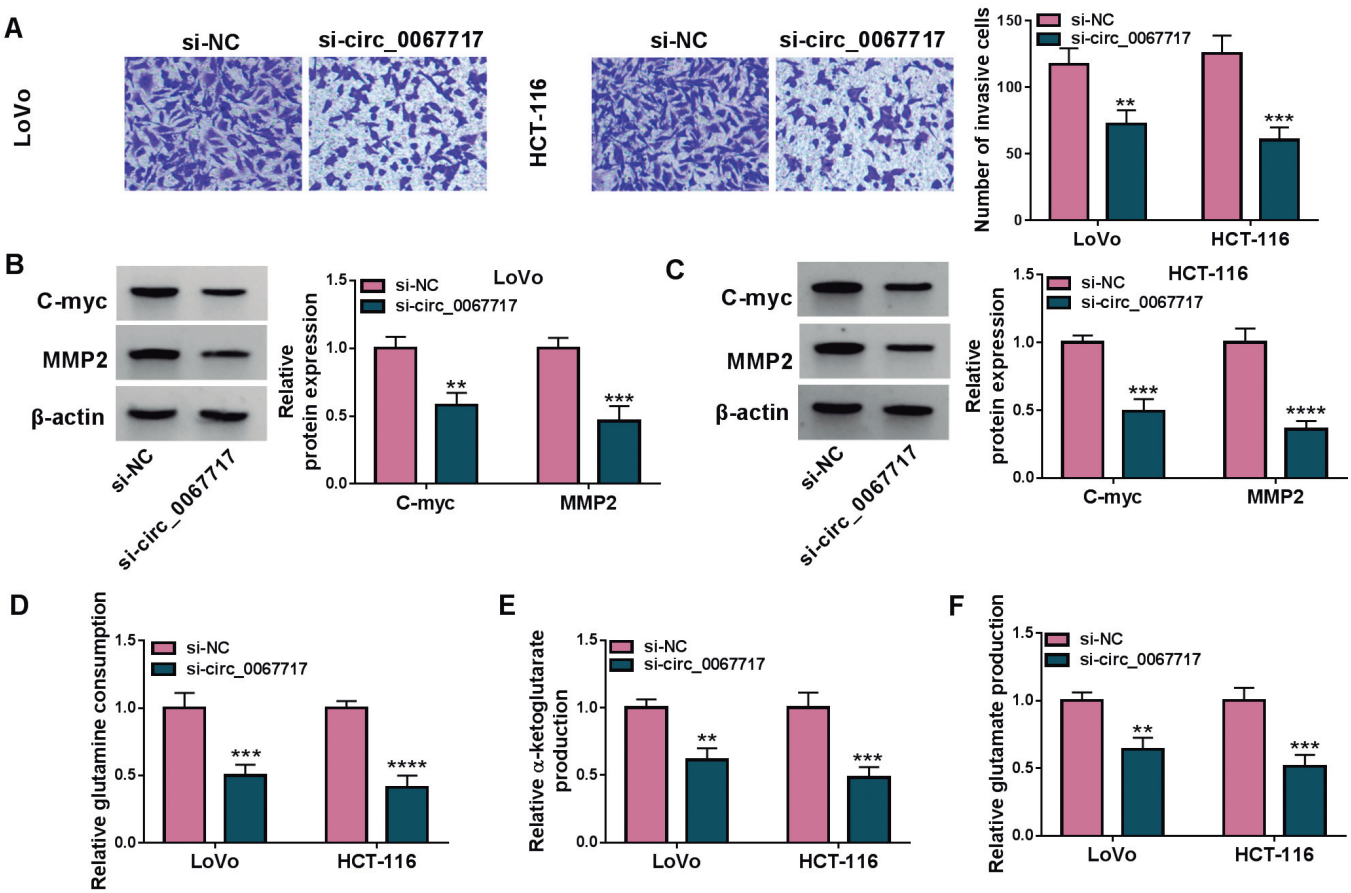


**Fig. 3.** The regulation of si-circ_0067717 on CRC cell invasion and glutamine metabolism. LoVo and HCT-116 cells were transfected with si-NC or si-circ_0067717. **A.** Transwell assay was used to examine cell invasion. **B, C.** C-myc and MMP2 protein levels were examined by WB analysis. **D-F.** Glutamine consumption, α-ketoglutarate production and glutamate production were used to evaluate cell glutamine metabolism. **P<0.01, ***P<0.001, ****P<0.0001.

circ_0067717 in CRC progression. After transfection, we confirmed that circ_0067717 expression was markedly reduced (Fig. 2A). CCK8 assay and EdU assay were used to assess cell proliferation, and the results showed that circ_0067717 knockdown repressed cell viability, and EdU positive cell rate in LoVo and HCT-116 cells (Fig. 2B,C). By detecting cell apoptosis using flow cytometry, we found that silenced circ_0067717 enhanced the apoptosis of CRC cells (Fig. 2D). After silencing circ_0067717, the invasion of LoVo and HCT-116 cells were reduced significantly (Fig. 3A). Also, the protein levels of proliferation marker C-myc and invasion marker MMP2 in LoVo and HCT-116 cells were also decreased by circ_0067717 downregulation (Fig. 3B,C). Glutamine is the most important nitrogen source and respiratory dye for cancer cells (Hensley et al., 2013; Cluntun et al., 2017). Therefore, a decrease in glutamine metabolism capacity may suggest that cancer cell growth is inhibited. Here, we measured glutamine consumption, α-ketoglutarate production and glutamate production to assess glutamine metabolism. The results showed that silenced circ_0067717 inhibited glutamine consumption, α-ketoglutarate production and glutamate production in LoVo and HCT-116 cells (Fig. 3D-F). The above data illuminated that circ_0067717 contributed to CRC progression.

### *Circ_0067717 served as a miR-497-5p sponge*

The starbase software was used to predict the targeted miRNA for circ_0067717. Through prediction, we selected 4 miRNAs (miR-107, miR-15a-5p, miR-195-5p and miR-497-5p) that have been studied in CRC as candidate miRNAs for circ_0067717. By detecting the expression of each miRNA, we found that the expression of miR-497-5p was most significantly affected by circ_0067717 knockdown (Fig. 4A,B). Therefore, miR-497-5p was selected as the target of circ_0067717 for research. The binding sites between miR-497-5p and circ_0067717 were shown in Figure 4C. Then, we constructed miR-497-5p mimic to overexpress miR-497-5p in LoVo and HCT-116 cells (Fig. 4D, 5.57-fold in LoVo cells and 4.55-fold in HCT-116 cells). After that, miR-497-5p mimic and WT/MUT-circ_0067717 vectors were transfected into CRC cells to perform dual-luciferase activity assay. As shown in Fig. 4E-F, miR-497-5p mimic only reduced the luciferase activity driven by the WT-circ_0067717 vector, confirming the interaction between miR-497-5p and circ_0067717. Through analyzing miR-497-5p expression using UALCAN software, miR-497-5p was observed to be lowly expressed in colon adenocarcinoma (COAD) tissues (Fig. 4G). Here, we detected that miR-

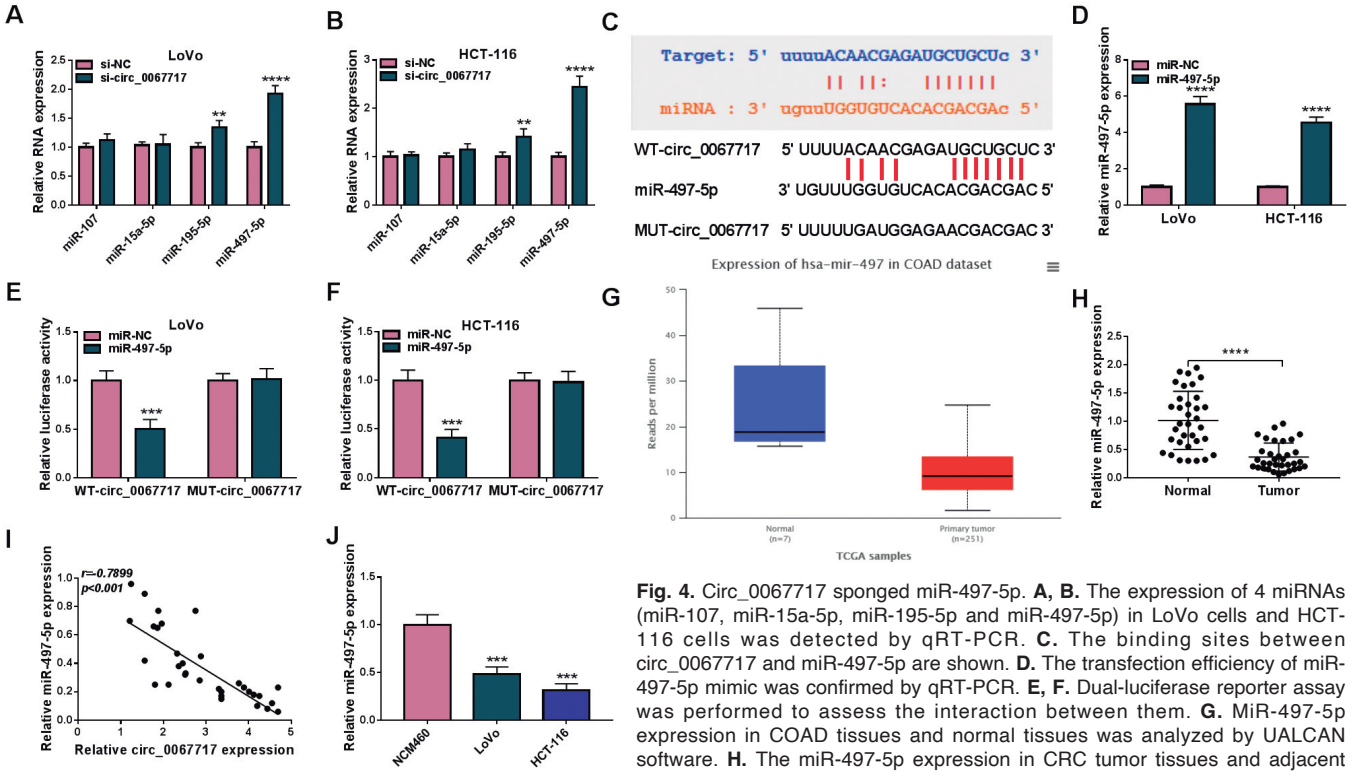


**Fig. 4.** Circ_0067717 sponged miR-497-5p. **A, B.** The expression of 4 miRNAs (miR-107, miR-15a-5p, miR-195-5p and miR-497-5p) in LoVo cells and HCT-116 cells was detected by qRT-PCR. **C.** The binding sites between circ_0067717 and miR-497-5p are shown. **D.** The transfection efficiency of miR-497-5p mimic was confirmed by qRT-PCR. **E, F.** Dual-luciferase reporter assay was performed to assess the interaction between them. **G.** MiR-497-5p expression in COAD tissues and normal tissues was analyzed by UALCAN software. **H.** The miR-497-5p expression in CRC tumor tissues and adjacent normal tissues was examined by qRT-PCR. **I.** Pearson correlation analysis was used to assess the correlation between miR-497-5p and circ_0067717. **J.** The expression of miR-497-5p in CRC cells (LoVo and HCT-116) and NCM460 cells was detected by qRT-PCR. **P<0.01, ***P<0.001, ****P<0.0001.

497-5p was downregulated in CRC tumor tissues, and its expression was negatively correlated with circ_0067717 expression (Fig. 4H,I). Meanwhile, the low expression of miR-497-5p was also found in CRC cells compared to NCM460 cells (Fig. 4J).

### *MiR-497-5p inhibitor reversed si-circ_0067717-mediated CRC cell progression*

In further experiments, si-circ_0067717 and anti-miR-497-5p were co-transfected into CRC cells. The detection results of miR-497-5p expression showed that circ_0067717 knockdown significantly increased miR-497-5p expression, while the addition of anti-miR-497-5p reversed this effect (Fig. 5A). Our data revealed that miR-497-5p inhibitor revoked the suppressive effect of circ_0067717 knockdown on cell viability and EdU positive cell rate (Fig. 5B,C). Also, si-circ_0067717-induced apoptosis in LoVo and HCT-116 cells was reversed by miR-497-5p inhibitor (Fig. 5D). Furthermore, we found that the inhibition effects of si-circ_0067717 on the number of invasive cells, the protein expression of C-myc and MMP2, glutamine consumption, α-ketoglutarate production and glutamate production in LoVo and HCT-116 cells were also overturned by anti-miR-497-5p (Fig. 5E-J). These data suggested that circ_0067717 sponged miR-497-5p to promote CRC progression.

### *MiR-497-5p targeted SLC7A5*

In the above studies, we confirmed that circ_0067717 could affect the process of glutamine metabolism, and further we speculated that circ_0067717/miR-497-5p axis might regulate the proteins related to glutamine metabolism. The starbase prediction revealed that miR-497-5p might target the glutamine metabolizing protein SLC7A5 (Fig. 6A), so SLC7A5 was selected as a target of miR-497-5p in further study. MiR-497-5p mimic reduced the luciferase activity of WT-SLC7A5 3'UTR vector, which confirming the interaction between miR-497-5p and

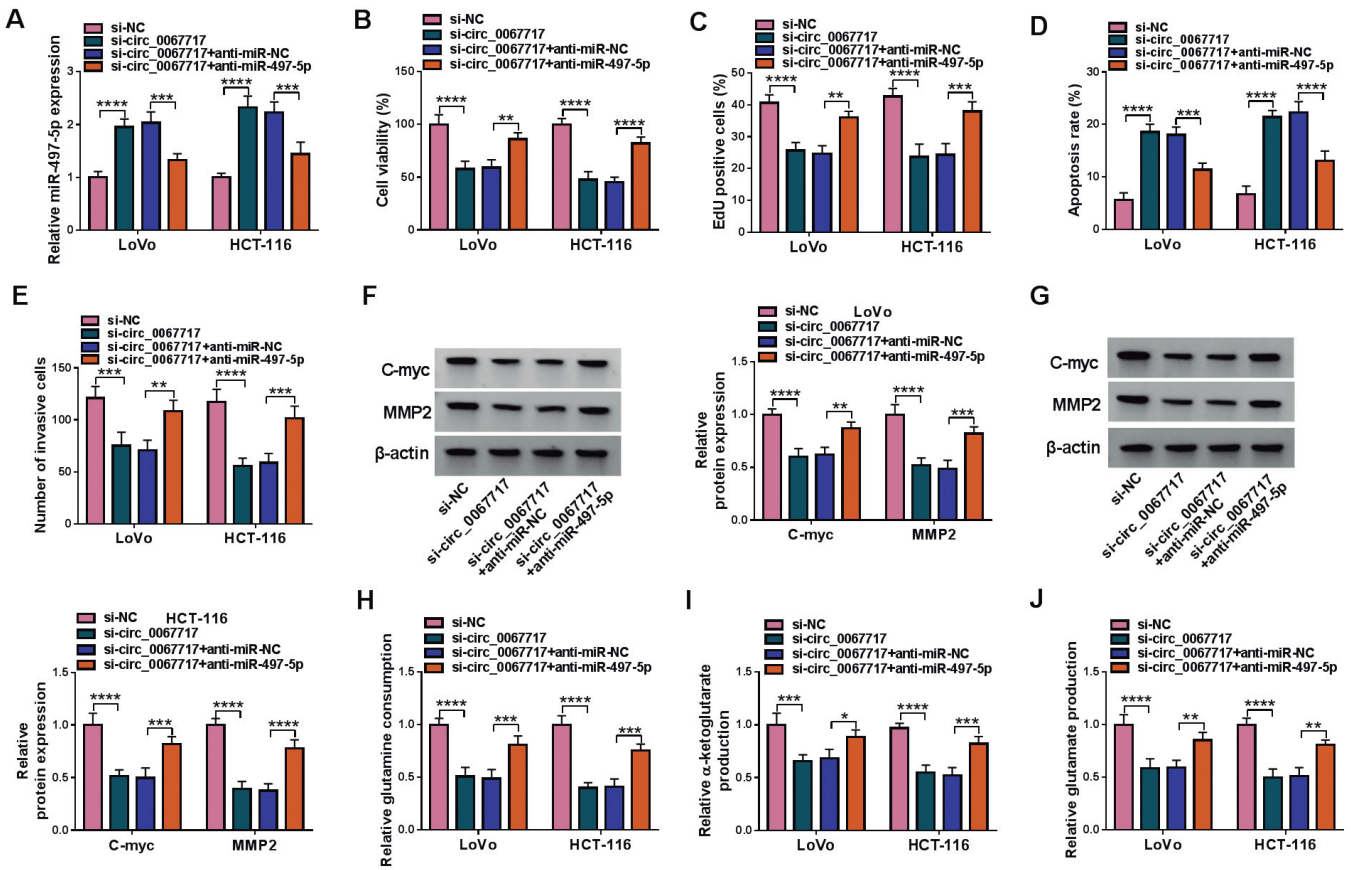


**Fig. 5.** The regulation of si-circ_0067717 and anti-miR-497-5p on CRC cell progression. LoVo and HCT-116 cells were transfected with si-circ_0067717 and anti-miR-497-5p. **A.** miR-497-5p expression was examined by qRT-PCR. Cell proliferation, apoptosis and invasion were determined using CCK8 assay **(B)**, EdU assay **(C)**, flow cytometry **(D)** and transwell assay **(E)**. **F, G.** WB analysis was used to determine the C-myc and MMP2 protein levels. **H-J.** Cell glutamine metabolism was analyzed by detecting glutamine consumption, α-ketoglutarate production and glutamate production. **P<0.01, ***P<0.001, ****P<0.0001.

SLC7A5 (Fig. 6B,C). In GEPIA database, SLC7A5 mRNA expression was found to be upregulated in COAD tissues (Fig. 6D). In TCGA samples, SLC7A5 expression was also discovered to be significantly upregulated in COAD tissues and remarkably overexpressed in different cancer stages (Fig. 6E). In our study, we confirmed that SLC7A5 was highly expressed in CRC tumor tissues, and its expression was negatively correlated with miR-497-5p expression (Fig. 6F-G). At the protein level, SLC7A5 expression was elevated in CRC tumor tissues and cells compared to the negative controls (Fig. 6H,I).

### *MiR-497-5p suppressed CRC progression by inhibiting SLC7A5 expression*

In the subsequent experiments, miR-497-5p mimic and SLC7A5 overexpression vector were co-transfected into CRC cells. The results showed that miR-497-5p overexpression could decrease SLC7A5 protein expression, and the addition of SLC7A5 overexpression vector abolished this effect (Fig. 7A). Function analysis showed that miR-497-5p overexpression inhibited cell viability, EdU positive cell rate and the number of invaded cells, while promoting apoptosis rate in LoVo and HCT-116 cells. However, these effects were reversed by SLC7A5 overexpression (Fig. 7B-E). Also, upregulated miR-497-5p suppressed the protein expression of C-myc and MMP2, while SLC7A5 overexpression overturned this effect (Fig. 7F,G). Furthermore, overexpressed SLC7A5 also eliminated the suppressing effects of miR-497-5p mimic on glutamine consumption, α-ketoglutarate production and glutamate production of LoVo and HCT-116 cells (Fig. 7H-J). The above results indicated that miR-497-5p targeted SLC7A5 to repress CRC progression.

### *Circ_0067717 regulated SLC7A5 expression by sponging miR-497-5p*

To perfect the hypothesis of circ_0067717/miR-497-5p/SLC7A5 axis, we explored the regulation of circ_0067717 on SLC7A5 expression. In LoVo and HCT-116 cells, we observed that circ_0067717 knockdown significantly reduced SLC7A5 protein expression, while these effects were reversed by miR-

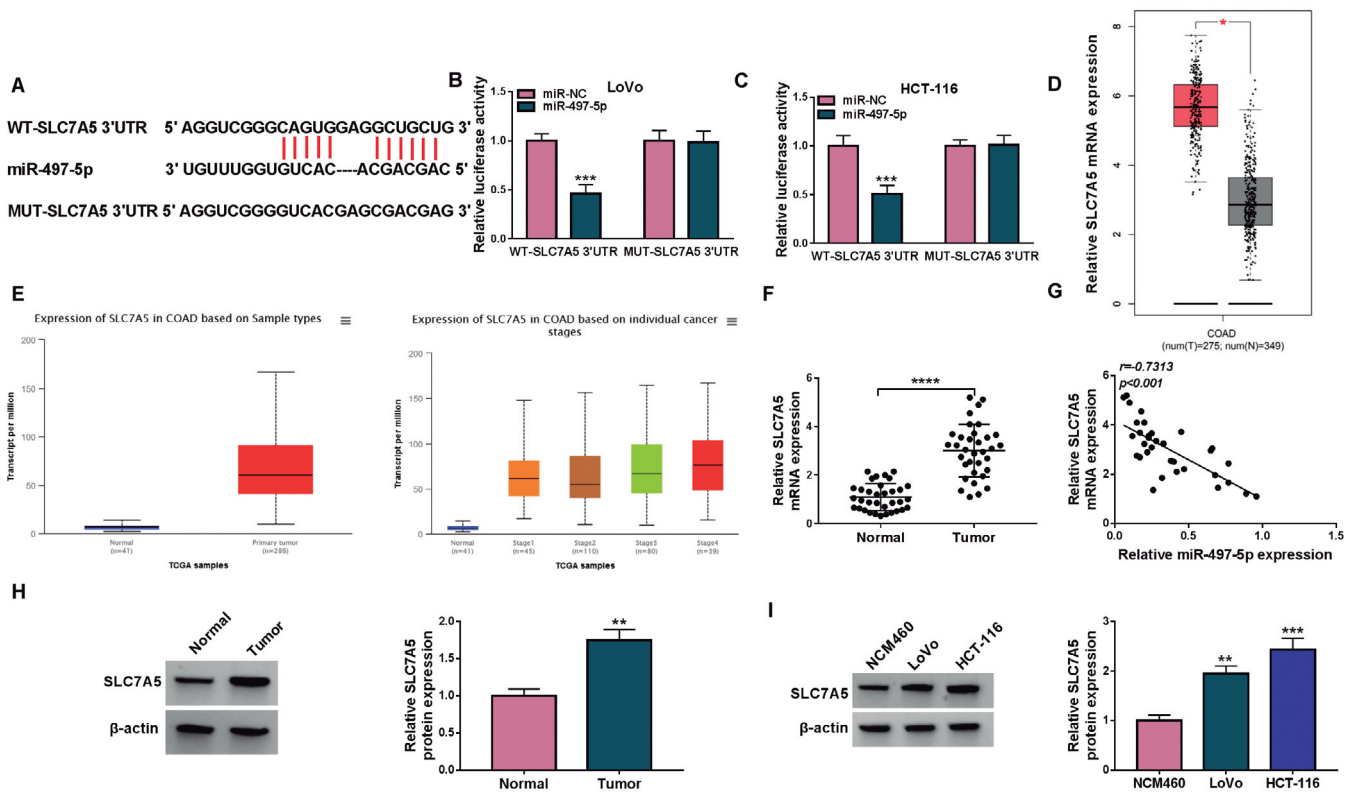


**Fig. 6.** MiR-497-5p targeted SLC7A5. **A.** The binding sites between miR-497-5p and SLC7A5 are shown. **B, C.** Dual-luciferase reporter assay was used to assess the interaction between them. **D.** In GEPIA database, SLC7A5 mRNA expression in COAD tissues and normal tissues was analyzed. **E.** SLC7A5 expression in COAD tissues and normal tissues was analyzed by UALCAN software. **F.** The SLC7A5 mRNA expression was examined by qRT-PCR in CRC tumor tissues and adjacent normal tissues. **G.** The correlation between miR-497-5p and SLC7A5 was analyzed by Pearson correlation analysis. **H, I.** The SLC7A5 protein expression in CRC tumor tissues and cells was detected by WB analysis. **P<0.01, ***P<0.001, ****P<0.0001.

497-5p inhibitor (Fig. 8A,B). Therefore, we confirmed that circ_0067717 sponged miR-497-5p to positively regulate SLC7A5.

### *Downregulated circ_0067717 inhibited CRC tumor growth in vivo*

In animal experiments, we found that tumor volume and weight were markedly reduced in the sh-circ_0067717 group compared to the sh-NC group (Fig. 9A,B). The expression of circ_0067717, miR-497-5p and SLC7A5 was measured in the tumor tissues of each group, and the results revealed that circ_0067717 expression and SLC7A5 protein level were decreased, while miR-497-5p expression was increased in the sh-circ_0067717 group (Fig. 9C,D). Also, the results of IHC staining showed that SLC7A5, C-myc and MMP2 positive cells were reduced in the tumor tissues of the sh-circ_0067717 group (Fig. 9E). Hence, our data verified that circ_0067717 might promote CRC tumorigenesis.

## Discussion

The occurrence and development of cancer involve complex pathological and physiological processes. CircRNAs abnormal expression has been discovered to be related to CRC cell growth, metastasis and other processes (Li et al., 2019; Zeng and Wang, 2020). Therefore, circRNA has unique advantages in becoming a potential biomarker for CRC treatment and diagnosis. Here, circ_0067717 function in CRC development was explored. The present results indicated that circ_0067717 had increased expression in CRC. Loss-of-function experiments illuminated that interference of circ_0067717 restrained CRC cell proliferation, invasion, glutamine metabolism, and accelerated apoptosis. Also, circ_0067717 knockdown restrained CRC tumorigenesis *in vivo*. The above data confirmed the oncogene role of circ_0067717 in CRC, which was

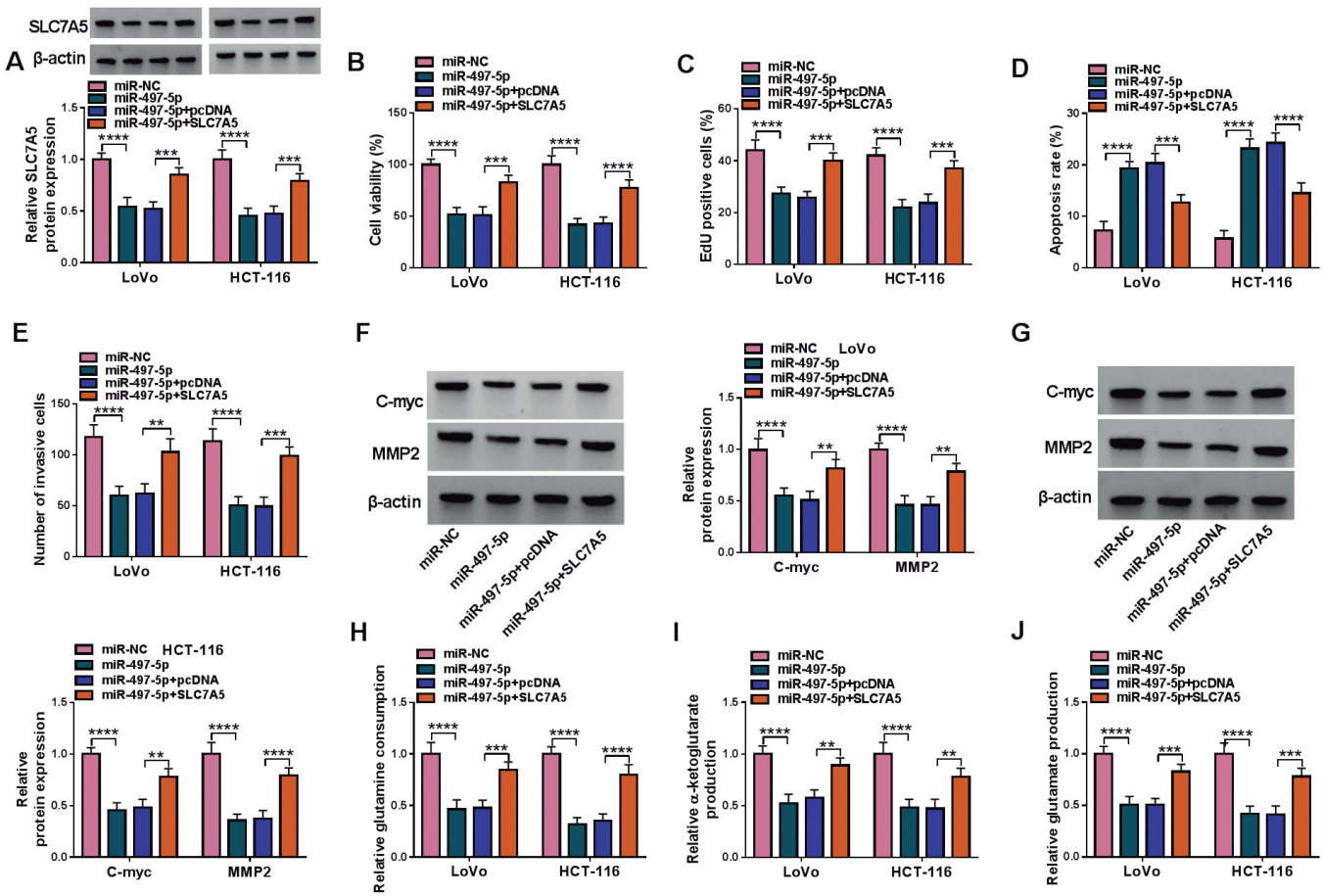


**Fig. 7.** The regulation of miR-497-5p and SLC7A5 on CRC cell progression. LoVo and HCT-116 cells were transfected with miR-497-5p mimic and SLC7A5 overexpression vector. **A.** The SLC7A5 protein expression was examined by WB analysis. CCK8 assay **(B)**, EdU assay **(C)**, flow cytometry **(D)** and transwell assay **(E)** were utilized for measuring cell proliferation, apoptosis and invasion. **F, G.** C-myc and MMP2 protein levels were examined using WB analysis. **H-J.** Cell glutamine metabolism was assessed by testing glutamine consumption, α-ketoglutarate production and glutamate production. **P<0.01, ***P<0.001, ****P<0.0001.

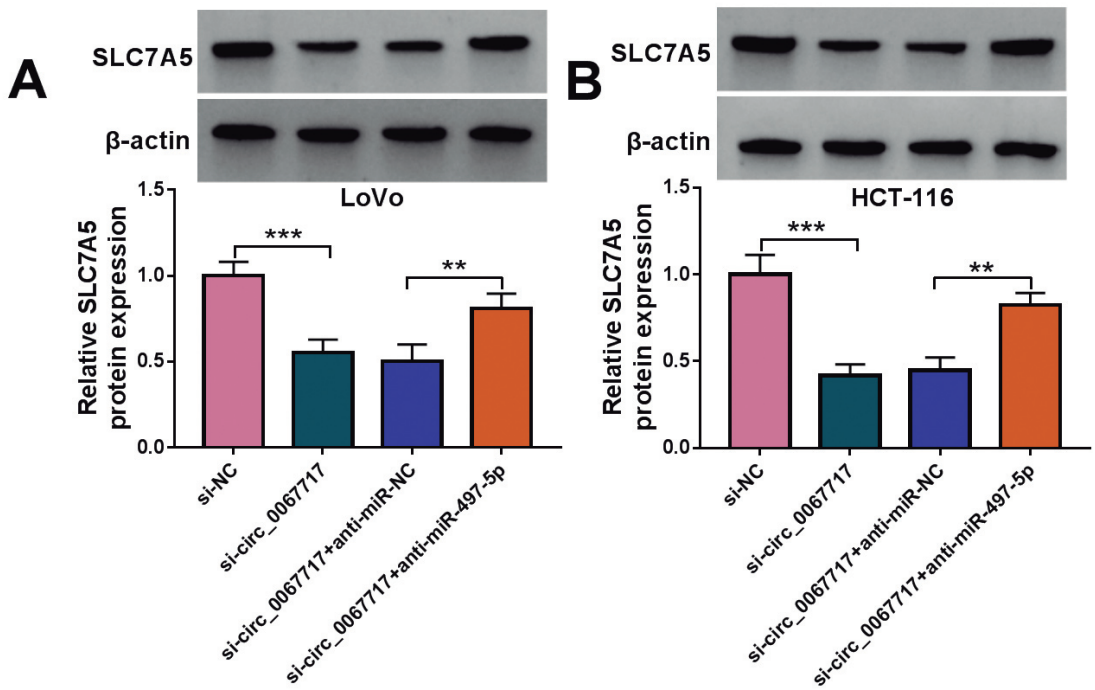


**Fig. 8.** Circ_0067717 and miR-497-5p regulated SLC7A5 expression. LoVo and HCT-116 cells were transfected with si-circ_0067717 and anti-miR-497-5p. The protein expression of SLC7A5 was measured by WB analysis in LoVo cells **(A)** and HCT-116 cells **(B)**. **P<0.01, ***P<0.001.

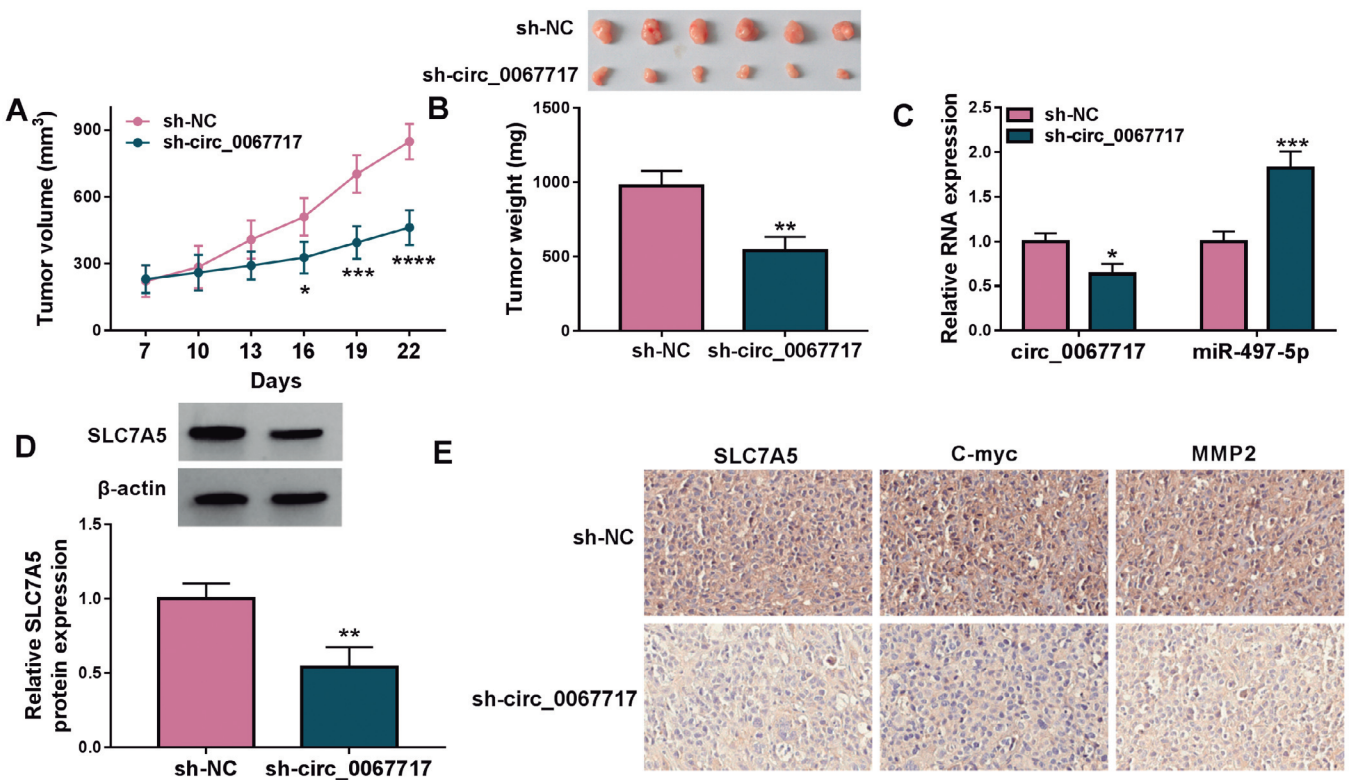


**Fig. 9.** The regulation of sh-circ_0067717 on CRC tumor growth in vivo. Tumor volume **(A)** and tumor weight **(B)** were measured. **C.** circ_0067717 and miR-497-5p expression in the tumor tissues of mice was analyzed by qRT-PCR. **D.** The SLC7A5 protein expression in the tumor tissues of mice was detected by WB analysis. **E.** IHC staining was used to analyze the SLC7A5, C-myc and MMP2 positive cells in the tumor tissues of mice. *P<0.05, **P<0.01, ***P<0.001.

consistent with its role in hepatocellular carcinoma (Chen et al., 2021).

MiR-497-5p was discovered to be sponged by circ_0067717. At present, the role of miR-497-5p in many cancers has been revealed. MiR-497-5p served as tumor suppressor to participate in regulating cancer development, including gastric cancer (Feng et al., 2019). Of course, many studies have shown that miR-497-5p also had an anti-tumor role in CRC malignancy progression. For example, miR-497-5p might repress cell growth and metastasis to hinder CRC progression (Wang et al., 2019). Besides, silenced miR-497-5p has been shown to promote CRC malignant phenotype through enhancing cell proliferation and metastasis (Yu and Zhang, 2020). In this, low miR-497-5p expression was found in CRC. Upregulation of miR-497-5p repressed CRC cell growth, invasion and glutamine metabolism, confirming the anti-cancer role of miR-497-5p in CRC. Additionally, anti-miR-497-5p abolished the regulation of si-circ_0067717 on CRC cell function, which further verified that miR-497-5p participated in circ_0067717-mediated CRC progression.

SLC7A5, also known as LAT1, is an important member of the L-type amino acid transporter (Najumudeen et al., 2021). SLC7A5 mutations block normal brain development and function, which may be related to its regulation on mTOR pathway activity (Sokolov et al., 2020). Oncogenic KRAS mutants increase glutamine metabolism to promote CRC cell proliferation, and targeted inhibition of SLC7A5 is an effective way to treat CRC with drug-resistant KRAS mutation (Najumudeen et al., 2021). Studies have shown that SLC7A5 is abnormally highly expressed in some tumor tissues and may play an important role in tumor progression (Bodoor et al., 2020; Kanai, 2021). Existing evidence showed that SLC7A5 was involved in gastric cancer development as a cancer-promoting factor, and its knockdown could inhibit cell metastasis (Wang et al., 2016). Also, SLC7A5 has been suggested to play a pro-proliferation role in breast cancer (Li et al., 2021) and lung cancer (Li et al., 2018). In CRC-related studies, SLC7A5 was considered to be an important independent marker associated with CRC patient's poor prognosis, and its expression was related to CRC cell proliferation and migration (Ogawa et al., 2019; Tang et al., 2021). Similar to the previous studies, the overexpressed SLC7A5 was confirmed in CRC tissues and cells. Functional analysis reported that overexpression of SLC7A5 rescued the phenotypes of CRC cells induced by miR-497-5p, verifying that miR-497-5p suppressed CRC malignant phenotype by targeting SLC7A5. Furthermore, we also confirmed the positive regulation of circ_0067717 on SLC7A5, which revealed that circ_0067717 served as a miR-497-5p sponge to upregulate SLC7A5.

In conclusion, the present study proposed a novel circRNA that regulated CRC progression. Circ_0067717 contributed to CRC growth, invasion and glutamine metabolism, which might depend on the miR-497-5p/SLC7A5 axis. The circ_0067717/miR-497-5p/SLC7A5 pathway provided a potential molecular target for CRC treatment, which has important clinical significance.

*Funding.* There is no funding to report.

*Conflict of interest.* The authors declare that they have no conflicts of interest.

## References

Araghi M., Soerjomataram I., Jenkins M., Brierley J., Morris E., Bray F. and Arnold M. (2019). Global trends in colorectal cancer mortality: projections to the year 2035. Int. J. Cancer 144, 2992-3000.

Arnold M., Sierra M.S., Laversanne M., Soerjomataram I., Jemal A. and Bray F. (2017). Global patterns and trends in colorectal cancer incidence and mortality. Gut 66, 683-691.

Bodoor K., Almomani R., Alqudah M., Haddad Y. and Samouri W. (2020). LAT1 (SLC7A5) overexpression in negative Her2 group of breast cancer: A potential therapy target. Asian Pac. J. Cancer Prev. 21, 1453-1458.

Carlomagno C., De Stefano A., Rosanova M., De Falco S., Attademo L., Fiore G. and De Placido S. (2019). Multiple treatment lines and prognosis in metastatic colorectal cancer patients. Cancer Metastasis Rev. 38, 307-313.

Chen Y., Li S., Wei Y., Xu Z. and Wu X. (2021). Circ-RNF13, as an oncogene, regulates malignant progression of HBV-associated hepatocellular carcinoma cells and HBV infection through ceRNA pathway of circ-RNF13/miR-424-5p/TGIF2. Bosn. J. Basic Med. Sci. 21, 555-568.

Cluntun A.A., Lukey M.J., Cerione R.A. and Locasale J.W. (2017). Glutamine metabolism in cancer: Understanding the heterogeneity. Trends Cancer 3, 169-180.

Feng L., Cheng K., Zang R., Wang Q. and Wang J. (2019). miR-497-5p inhibits gastric cancer cell proliferation and growth through targeting PDK3. Biosci. Rep. 39, BSR20190654.

Ge J., Jin Y., Lv X., Liao Q., Luo C., Ye G. and Zhang X. (2019). Expression profiles of circular RNAs in human colorectal cancer based on RNA deep sequencing. J. Clin. Lab. Anal. 33, e22952.

Geng F., Wang Z., Yin H., Yu J. and Cao B. (2017). Molecular targeted drugs and treatment of colorectal cancer: Recent progress and future perspectives. Cancer Biother. Radiopharm. 32, 149-160.

Hensley C.T., Wasti A.T. and DeBerardinis R.J. (2013). Glutamine and cancer: cell biology, physiology, and clinical opportunities. J. Clin. Invest. 123, 3678-3684.

Kanai Y. (2022). Amino acid transporter LAT1 (SLC7A5) as a molecular target for cancer diagnosis and therapeutics. Pharmacol. Ther. 230, 107964.

Kristensen L.S., Andersen M.S., Stagsted L.V.W., Ebbesen K.K., Hansen T.B. and Kjems J. (2019). The biogenesis, biology and characterization of circular RNAs. Nat. Rev. Genet. 20, 675-691.

Li C., He X., Zhang L., Li L. and Zhao W. (2019). A pair-wise meta-analysis highlights circular RNAs as potential biomarkers for colorectal cancer. BMC Cancer 19, 957.

Li H., Chen S., Liu J., Guo X., Xiang X., Dong T., Ran P., Li Q., Zhu B., Zhang X., Wang D., Xiao C. and Zheng S. (2018). Long non-coding RNA PVT1-5 promotes cell proliferation by regulating miR-

126/SLC7A5 axis in lung cancer. Biochem. Biophys. Res. Commun. 495, 2350-2355.

Li S. and Han L. (2019). Circular RNAs as promising biomarkers in cancer: detection, function, and beyond. Genome Med. 11, 15.

Li J., Sun D., Pu W., Wang J. and Peng Y. (2020). Circular RNAs in cancer: Biogenesis, function, and clinical significance. Trends Cancer 6, 319-336.

Li Y., Wang W., Wu X., Ling S., Ma Y. and Huang P. (2021). SLC7A5 serves as a prognostic factor of breast cancer and promotes cell proliferation through activating AKT/mTORC1 signaling pathway. Ann. Transl. Med. 9, 892.

Misir S., Hepokur C., Aliyazicioglu Y. and Enguita F.J. (2020). Circular RNAs serve as miRNA sponges in breast cancer. Breast Cancer 27, 1048-1057.

Najumudeen A.K., Ceteci F., Fey S.K., Hamm G., Steven R.T., Hall H., Nikula C.J., Dexter A., Murta T., Race A.M., Sumpton D., Vlahov N., Gay D.M., Knight J.R.P., Jackstadt R., Leach J.D.G., Ridgway R.A., Johnson E.R., Nixon C., Hedley A., Gilroy K., Clark W., Malla S.B., Dunne P.D., Rodriguez-Blanco G., Critchlow S.E., Mrowinska A., Malviya G., Solovyev D., Brown G., Lewis D.Y., Mackay G.M., Strathdee D., Tardito S., Gottlieb E., Consortium C.R.G.C., Takats Z., Barry S.T., Goodwin R.J.A., Bunch J., Bushell M., Campbell A.D. and Sansom O.J. (2021). The amino acid transporter SLC7A5 is required for efficient growth of KRAS-mutant colorectal cancer. Nat. Genet. 53, 16-26.

Ogawa H., Kaira K., Motegi Y., Yokobori T., Takada T., Katoh R., Osone K., Takahashi R., Katayama C., Oyama T., Kanai Y., Yao T., Asao T., Kuwano H. and Shirabe K. (2019). Role of amino acid transporter expression as a prognostic marker in patients with surgically resected colorectal cancer. Anticancer Res. 39, 2535-2543.

Panda A.C. (2018). Circular RNAs act as miRNA sponges. Adv. Exp. Med. Biol. 1087, 67-79.

Piawah S. and Venook A.P. (2019). Targeted therapy for colorectal cancer metastases: A review of current methods of molecularly targeted therapy and the use of tumor biomarkers in the treatment of metastatic colorectal cancer. Cancer 125, 4139-4147.

Shan T., Chen S., Chen X., Lin W., Li W., Ma J., Wu T., Cui X., Li W., Kang Y. and Yang W. (2019). Association of family history of tumors with clinicopathological characteristics and prognosis of colorectal cancer. Eur. J. Cancer Prev. 28, 258-267.

Sokolov A.M., Holmberg J.C. and Feliciano D.M. (2020). The amino acid transporter Slc7a5 regulates the mTOR pathway and is required for granule cell development. Hum. Mol. Genet. 29, 3003-3013.

Tang S., Liu Q. and Xu M. (2021). LINC00857 promotes cell proliferation and migration in colorectal cancer by interacting with YTHDC1 and stabilizing SLC7A5. Oncol. Lett. 22, 578.

Wang J., Fei X., Wu W., Chen X., Su L., Zhu Z. and Zhou Y. (2016). SLC7A5 functions as a downstream target modulated by CRKL in metastasis process of gastric cancer SGC-7901 cells. PLoS One 11, e0166147.

Wang H., Yu M., Hu W., Chen X., Luo Y., Lin X., Zeng Y. and Yao X. (2019). Linc00662 promotes tumorigenesis and progression by regulating miR-497-5p/AVL9 axis in colorectal cancer. Front. Genet. 10, 1385.

Wang S., Zhang K., Tan S., Xin J., Yuan Q., Xu H., Xu X., Liang Q., Christiani D.C., Wang M., Liu L. and Du M. (2021). Circular RNAs in body fluids as cancer biomarkers: the new frontier of liquid biopsies. Mol. Cancer 20, 13.

Wu M., Kong C., Cai M., Huang W., Chen Y., Wang B. and Liu X. (2021). Hsa_circRNA_002144 promotes growth and metastasis of colorectal cancer through regulating miR-615-5p/LARP1/mTOR pathway. Carcinogenesis 42, 601-610.

Xu H., Liu Y., Cheng P., Wang C., Liu Y., Zhou W., Xu Y. and Ji G. (2020). CircRNA_0000392 promotes colorectal cancer progression through the miR-193a-5p/PIK3R3/AKT axis. J. Exp. Clin. Cancer Res. 39, 283.

Yu C. and Zhang F. (2020). LncRNA AC009022.1 enhances colorectal cancer cells proliferation, migration, and invasion by promoting ACTR3B expression via suppressing miR-497-5p. J. Cell. Biochem. 121, 1934-1944.

Zeng K. and Wang S. (2020). Circular RNAs: The crucial regulatory molecules in colorectal cancer. Pathol. Res. Pract. 216, 152861.

Accepted July 12, 2022